Egyptian Journal of Chemistry

http://ejchem.journals.ekb.eg/

Isolation and Structure Elucidation of Aromatic Polyketides from Marine Actinomycete with Antibiofilm Activity against *Staphylococcus aureus* and *Escherichia coli*

Aya R. Badran [a], Sally A. Ali [b], Hassan Y. Ebrahim [c], Ali M. S. Hebishy [a],
Ehab A. Essawy [a], and Mohamed S. Abdelfattah [a]*

[a] *Chemistry Department, Faculty of Science, Helwan University, Cairo 11795, Egypt*
[b] *Botany and Microbiology Department, Faculty of Science, Helwan University, Cairo 11795, Egypt*
[c] *Faculty of Pharmacy, Helwan University, Ain Helwan, Cairo 11795, Egypt*

Abstract

Three pigmented secondary metabolites tetracenomycin D (**1**), resistomycin (**2**), and resistoflavin (**3**) were isolated from *Streptomyces* sp. EG1 and their antibiofilm activities were evaluated against *Staphylococcus aureus* and *Escherichia coli*. The isolated compounds were purified by different chromatographic methods, including Silica gel and Sephadex LH-20, and their chemical structures were elucidated by mass and NMR spectroscopy. Tetracenomycin D (**1**) inhibited 75% of both pathogens from creating biofilm at 400 µg/ml, whereas resistomycin (**2**), and resistoflavin (**3**) inhibited biofilm by more than 80% at the same concentration. The light microscopic investigation revealed that compounds **1**-**3** inhibit the formation of biofilms and the adhesion of bacterial cells to the surface of glass pieces. As observed by confocal laser scanning microscopy (CLSM), pigmented metabolites **1**-**3** disrupt the 3D architecture of biofilm-forming bacteria. Molecular docking was used to find out how compounds **1**–**3** bind to the active sites of the biofilm-forming proteins ClfB and CsgG in *S. aureus* and *E. coli*, respectively.

Keywords: actinomycetes; antibiofilm; light microscope; confocal laser scanning microscope; ClfB; CsgG; molecular docking

1. Introduction

Many pathogenic bacteria congregate in the natural environment to obtain food and remain alive [1–3]. These pathogens can adapt to changes in their surroundings by forming biofilms, which are made up of a combination of polymeric components, most of which are polycarbohydrates, mutually known as extracellular polymeric substances (EPS), as well as proteins, lipids, eDNA, and other biomaterials [4,5]. The biofilms must first adhere to a surface of wet and dry unsterilized moiety and then multiply to form microcolonies, each containing a single or several species of microorganisms [5–7]. Colonization and consequent formation of biofilms can occur in different places such as health care centers, clinics, hospitals, and surfaces of medical equipment (e.g., heart valves, pacemakers, drains, surgical pins, prostheses, contact lenses, etc.) [8,9]. Furthermore, biofilms are found in the infected wounds, human skin's surface, and the gastrointestinal tract [10–12].

Many bacterial species, including Gram-positive (i.e., *Staphylococcus aureus*) and Gram-negative infections (i.e., *Escherichia coli*), are capable of generating biofilms [13,14], which are substantially more resistant to antibiotics than free-living pathogens, as bacteria susceptible to antimicrobial drugs may become resistant after biofilm formation [15]. According to findings from several studies, biofilms may be involved in most bacterial infectious diseases and the body's chronic infections [16,17]. As a result, more collaborative efforts of scientists in developing and discovering antimicrobial agents to inhibit or eliminate bacterial biofilm formation are required. In this regard, microorganisms constitute a valuable source of biologically active compounds for developing therapeutic agents [18–21]. However, marine actinomycetes have been the dominant source of promising compounds with antimicrobial activity [22,23]. It has been discovered that several species of actinomycetes produce compounds that impede the biofilm formation of *S. aureus and E. coli* [24,25]. For example, marine *Streptomyces variabilis* was discovered to produce 1-hydroxy-1-norresistomycin (HNM) [26]. In this study, we isolated three pigmented secondary metabolites of tetracenomycin

D (**1**), resistomycin (**2**), and resistoflavin (**3**) from the culture of marine *Streptomyces* sp. EG1 and evaluated their effects on *S. aureus and E. coli* biofilm formation. Furthermore, molecular docking was used to identify the structural features of these compounds with the binding sites of biofilm-forming proteins ClfB and CsgG in *S. aureus* and *E. coli*, respectively.

2. Experimental

All chemicals, reagents and solvents used in the study were purchased from Sigma Aldrich without any additional purification. All NMR data were measured using Bruker Avance III™ HD 500 MHz. The biofilm was observed using Confocal Laser Scanning Microscopy (CLSM) LSM 710, Software version ZEN 2.3. The manufacturing company was Carl Zeiss (ZEISS) (Carl Zeiss, Jena, Germany).

2.1. Fermentation, extraction, and isolation of compounds from Streptomyces sp. EG1

The *Streptomyces* sp. EG1 was isolated from a sediment sample collected from the northern Egyptian coast along the Mediterranean Sea, using a serial dilution method on starch-casein agar plates. In brief, one gram of wet sediment was dispersed in 9 mL of sterilized water and subjected to heating at 60°C for 10 min. A serial dilution (10^{-1}, 10^{-2} and 10^{-3}) of the suspension with sterilised seawater was carried, and an aliquot (100 μL) was spread on a starch-casein agar plate. The strain was given voucher EG1 and identified as a *Streptomyces* sp. by 16S rRNA gene sequence analysis (GenBank accession no. MT186138) [22]. The strain was cultivated at 28°C for 72 hours on four Waksman agar medium containing glucose 2.0 g, meat extract 0.5 g, peptone 0.5 g, dried yeast 0.3 g, NaCl 0.5 g, $CaCO_3$ 0.3 g, and agar 1.5 g in 100 ml water. A small pieces of agar were used to inoculate 100×250 cm^3 Erlenmeyer flasks, each with 100 ml of Waksman medium (WM). Fermentation was carried out at a temperature of 28°C for 7 days and a shaking speed of 200 rpm. The culture broth was centrifuged at 3000 rpm for 15 min, and the resulting mycelia were extracted three times with methanol (3×0.5 L) and concentrated under reduced pressure. The fermentation broth was extracted with ethyl acetate three times and concentrated under a vacuum. As the TLC of both broth and mycelia contained our target compounds, they were combined to give 3.67 g of brown crude extract. The extract was chromatographed on a silica gel column, using stepwise elution with dichloromethane (DCM) and methanol (MeOH) to give eight fractions. Fraction **2** was purified by PTLC coated with silica gel (8 plates, 20×20 cm, DCM/7%MeOH) to give tetracenomycin D (**1**, 10 mg), and resistomycin (**2,** 25 mg) as red and orange powders, respectively. Fraction **3** was

subjected to Sephadex LH-20 (4×120 cm, MeOH) followed by PTLC (4 plates, 20×20 cm, DCM/10%MeOH) to give 5.0 mg of resistoflavin (**3**).

2.2. Spectroscopic data of compounds 1-3

Tetracenomycin D (1): red solid; ^{1}H NMR (500 MHz, DMSO-d_6): δ_H 7.79 (1H, s, H-6),7.09(1H, brd, H-7),7.06(1H, d, *j*=2.4, H-4),6.91(1H, brd *j*=1.9, H-9),6.51(1H, d, *j*=2.4, H-2),2.75(3H, S, H-13); ^{13}C NMR (125 MHz, DMSO-d_6): δ_C188.3 (C-12), 180.9(C-5), 166.1 (C-11), 165.1 (C-3),164.3 (C-1),159.8 (C-8),141.4 (C-10) ,139.9 (C-6a), 135.7 (C-4a), 127.8 (C-5a), 123.4 (C-9), 121.5 (C-6),119.4 (C-10a), 111.6 (C-7), 109.6 (C-12a), 108.1 (C-4), 108 (C-2),106.5 (C-11a), 24.5 (C-13); ESI-MS: m/z 337.0 [M+H]$^+$

Resistomycin (2): orange solid; ^{1}H NMR (500MHz, DMSO-d_6): δ_H 1.55 (6H, s, Me-1), 2.88 (3H, s, Me-9), 6.32 (1H, s, H-4), 6.98 (1H, s, H-8), 7.24(1H, s, H-11), 11.94 (1H, s, OH-10), 13.98 (1H, s, OH-5), 14.33 (1H, s, OH-3), 14.48 (1H, s, OH-7);^{13}C NMR (125 MHz, DMSO-d_6):δ_C 26.0 (Me-9), 28.8 (Me-1), 46.3 (C-1), 100.5 (C-4), 102.8 (C-2a), 106.1 (C-5a), 107.0 (C-6a), 107.3 (C-11b), 110.5 (C-11), 114.4 (C-9a), 119.6 (C-8), 129.0(C-9b), 139.9 (C-11c), 152.4 (C-9), 152.9 (C-11a), 163.7 (C-10), 168.2 (C-7), 170.1(C-5), 170.6 (C-3), 179.2 (C-6), 205.2 (C-2). ESI-MS: m/z 377.0 [M+H]$^+$.

Resistoflavin (3): orange solid; ^{1}H NMR (500 MHz, DMSO-d_6): δ_H 13.35 (OH), 12.63 (OH), 12.35 (OH), 7.29 (OH), 6.97 (1H, s, H-8), 6.52 (1H, s, H-4), 6.47 (1H, s, H-11), 2.76 (3H, s, H-14), 1.61 (3H, s, H-12), 1.54 (3H, s, H-13); 13C NMR (500 MHz, DMSO-d6): δ_C 203.6 (C-2), 189.2 (C-6), 183.7 (C-10), 168.4 (C-5 and C-7), 163.9 (C-3), 156.6 (C-11a), 150.1 (C-9), 149.5 (C-11c), 148.4 (C-11d), 127.7 (C-11), 121.2 (C-8), 120.5 (C-9a), 111.6 (C-6a), 108.6 (C-5a), 107.6 (C-2a), 104.4 (C-4), 62.0 (C-11b), 46.7 (C-1), 31.2 (C-12), 24.4 (C-13), 23.7 (C-14); ESI-MS: m/z 393.0 [M+H]$^+$.

2.3. Biofilm inhibition assay for compounds 1-3

The antibiofilm activity of tetracenomycin D (**1**), resistomycin (**2**), and resistoflavin (**3**) was performed in a 96-well microtiter plate using the crystal violet staining assay [27,28]. The pathogenic bacteria, *Staphylococcus aureus* LC189114 and *Escherichia coli* OK087362 that produce the biofilm were cultured overnight in nutrient broth medium (NBM) at 37°C. The bacterial cultures of each pathogen were diluted with fresh NBM to an optical density of 0.2. The negative control was sterilized nutrient broth medium (NBM) cultured overnight. A 100 μl of dilutions were incubated with each compound at different concentrations (100, 200, 300, and 400 μg/ml) in polystyrene round bottom 96 well plates. After inoculating the plate at 37°C for 72

hours, the contents were discarded, and the wells were washed twice with phosphate-buffered saline (PBS) to remove bacteria that were not tightly bound. The biofilms were dyed for 30 minutes with 100 µl of 0.1% crystal violet solution (w/v), after which the dye was removed, and the wells were washed twice with deionized water. The wells were allowed to dry before the dye was solubilized in 100 µl of absolute ethanol, and the optical density at 630 nm was measured using a microplate reader (ChroMate 4300). The percentage of biofilm inhibition was calculated as follows:

Biofilm inhibition (%) = (Control OD_{630}-Treatment OD_{630}/ Control OD_{630}) × 100

2.4. Light microscopic analysis

The inhibition of biofilms formed by *E. coli* and *S. aureus* after treatment with compounds **1**-**3** was observed by a light microscope (Optika Microscope, Italy) [26]. A culture without compounds served as a negative control. In brief, biofilms were allowed to adhere to the surface of sterile circular glass coverslips (5 mm in diameter) in a 96-well polystyrene microtiter plate treated with and without tetracenomycin D (**1**), resistomycin (**2**), and resistoflavin (**3**) at a concentration of 400 µg/ml. After incubating at 37°C for 24 h, the glass pieces were rinsed with PBS and dyed with 0.1% crystal violet. The stained-glass pieces were placed on slides with the biofilm pointed upwards and viewed under a light microscope at a magnification of 40X. A digital camera connected to the light microscope captured the visible biofilms.

2.5. Confocal laser scanning microscopy (CLSM) analysis

To observe the effect of tetracenomycin D (**1**), resistomycin (**2**), and resistoflavin (**3**) on the three-dimensional architecture of biofilm formation, we used a confocal laser scanning microscope (LSM 710, Carl Zeiss, Jena, Germany). Cell suspensions (1%) of *S. aureus* and *E. coli* and were mixed with 100 µl of NBM and put into 96-well sterile polystyrene microtiter plates containing sterilized coverslips 400 µg/ml of compounds **1**-**3**. The plates were incubated at 37°C for 24 h, and the adhered biofilm was stained with the fluorescent acridine orange dye and kept for an extra 10 min in a dark place. The coverslips were carefully washed two times with PBS to remove the excess acridine orange dye and then investigated with a CLSM. The biofilm grown on the coverslips that didn't have the compounds **1**-**3** was used as a control. To investigate the biofilm inhibition efficacy, three-dimensional (3D) images were captured, and Z-stacks were created to assess biofilm thickness [29].

2.6. Molecular modelling

The interactions of tetracenomycin D (**1**), resistomycin (**2**), and resistoflavin (**3**) with the ClfB and CsgG proteins of *S. aureus* and *E. coli*, respectively, were determined using molecular docking analysis. We used the Chemical Computing Group's Molecular Operating Environment (MOE) 2014.09 release. The manipulated X-ray crystal structures of *Staphylococcus aureus* clumping factor B (ClfB) ligand-binding domain (PDB code: 4F27) and the *E. coli* curli membrane protein subunit CsgG (PDB code: 6L7C) were retrieved from the Protein Data Bank and used in all docking experiments. The structure preparation application of MOE was used to prepare enzyme complexes, where structural issues such as alternates, termini, hydrogen count, and incorrect charges have been addressed and corrected. Protonate 3D was used to discover residues as rotamers, protomers, or tautomers. Energy minimization was performed using a preset MMFF94x force field. The 2D structures of the aromatic polyketide tetracenomycin D (**1**), resistomycin (**2**), and resistoflavin (**3**) were sketched, utilizing the ChemDraw User Interface version 15.0, and were saved as MDL Molfile. Structures were then imported onto the MOE interface, and the 3D structures of the molecules were generated for conformational search. The geometry optimization and energy minimization were implemented for generated 3D structures. The rigid receptor docking protocol was implemented for docking studies, using the Triangle Matcher for Placement and the London dG for Rescoring and Force Field for Refinement.
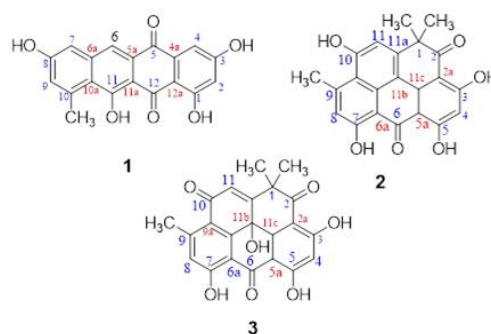
3. Results and discussion
3.1. Production of compounds 1-3 and evaluation of their antibiofilm activity

The marine *Streptomyces* sp. EG1 was isolated from Egypt's Mediterranean shore near Mersa Matruh City and fermented on a 10-liter scale using Waksman medium at 28°C for 7 days with a shaking speed of 200 rpm. After extraction and evaporation, the crude extract was fractionated by silica gel column chromatography to give eight fractions, which were purified to yield tetracenomycin D (**1**), resistomycin (**2**), and

resistoflavin (**3**). The chemical structures of compounds **1**-**3** (Figure 1) were established using NMR spectroscopy and by comparison with our authentic samples [30,31].

The isolated metabolites **1**-**3** were evaluated for their ability to suppress the formation of biofilms in *E. coli* and *S. aureus* using a crystal violet staining assay at various concentrations (100–400 µg/ml). The biofilms produced by both tested pathogens are Fig. 1. Metabolites isolated from *Streptomyces* sp. EG1

significantly reduced as the concentration of metabolites **1**-**3** increases (Figure 2), with 200 µg/ml considered the biofilm inhibitory concentration (BIC$_{50}$). Compound **1** inhibited biofilm formation in *S. aureus* and *E. coli* by more than 75% at 400 µg/ml, while compounds **2** and **3** inhibited biofilm formation by greater than 80% at the same concentration. It was also observed that biofilm inhibition activity for tetracenomycin D (**1**) and resistomycin (**2**) at different concentrations against *E. coli* is greater than that of *S. aureus*, which contrasts with resistoflavin (**3**) at 300 and 400 µg/ml. Ramalingam *et al.* studied the antibiofilm activity of the similar derivative 1-hydroxy-1-norresistomycin (HNM) against different clinical pathogens, including *E. coli*, *V. cholerae,* and *S. aureus* [26]. They found that HNM at a 200 µg/ml concentration inhibited the biofilm formation of their tested clinical pathogens by more than 92%. Previous study also found that anthraquinone derivatives isolated from the actinobacteria *Kitasatospora albolonga* were effective antibiofilm agents against methicillin-resistant *Staphylococcus aureus* (MRSA) [32].

3.2. Microscopic visualization of the tested pathogens biofilms

The effect of compounds **1**-**3** on biofilm formation of *S. aureus* and *E. coli* was observed by light microscopy and confocal laser scanning microscopy (CLSM). The light microscope (Figure 3) showed that the biofilms without pigmented compounds had typical morphologies and dense structures. When tetracenomycin D (**1**), resistomycin (**2**), and resistoflavin (**3**) were incubated with the tested pathogens at 200 µg/ml for 24 h, a reduction in biofilm formation, structural alterations, and scattered appearance were observed. CLSM images in 2D, ortho, and 3D also revealed that compounds **1**-**3** reduced the thickness of biofilms, and their structural morphology had been changed with a reduced number of micro-colonies in *S. aureus* and *E. coli* compared to the controls (Figures 4 and 5).

3.3. Molecular docking

To investigate the binding modes of tetracenomycin D (**1**), resistomycin (**2**), and resistoflavin (**3**) with the active sites of clumping

factor B (ClfB), expressed in *S. aureus* [33] and CsgG found in *E. Coli* [34,35], molecular docking was performed by Molecular Operating Environment (MOE) 2014.09 release. These two proteins characterized both pathogens' microbial cell surface adhesions [34,36]. The X-ray structures of ClfB and CsgG were retrieved from the Protein Data Bank and then prepared for the subsequent computational studies (Figure 6).

As depicted in Figure 6, the ClfB ligand binding component comprises two distinct *N*-terminal N2 and N3 domains previously described for microbial surface components recognizing adhesive matrix molecules (MSCRAMM) family [37]. The N2 and N3 domains have two layers of tightly packed β-sheets, while the packing between the two domains is relatively slacked, resulting in the formation of a binding trench between N2 and N3 domains, presumably for ligands binding. On the other hand, CsgG's crystal structure shows a tightly connected, symmetrical nonamer that looks like a crown and has a channel in the middle.
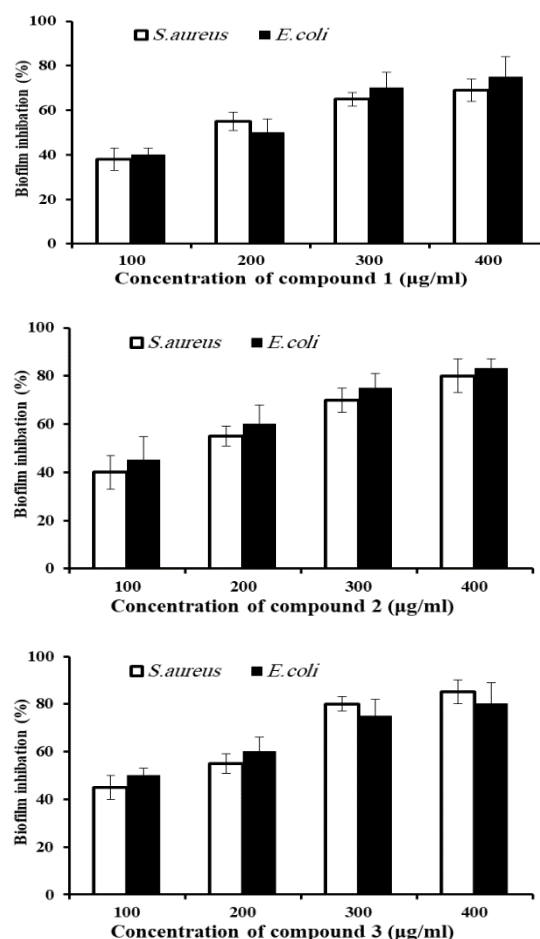

Fig. 2. Antibiofilm activity of tetracenomycin D (**1**), resistomycin (**2**), and resistoflavin (**3**) against *S. aureus* and *E. coli* biofilm inhibition at different concentrations. Error bars indicated the standard deviation of three replicates.
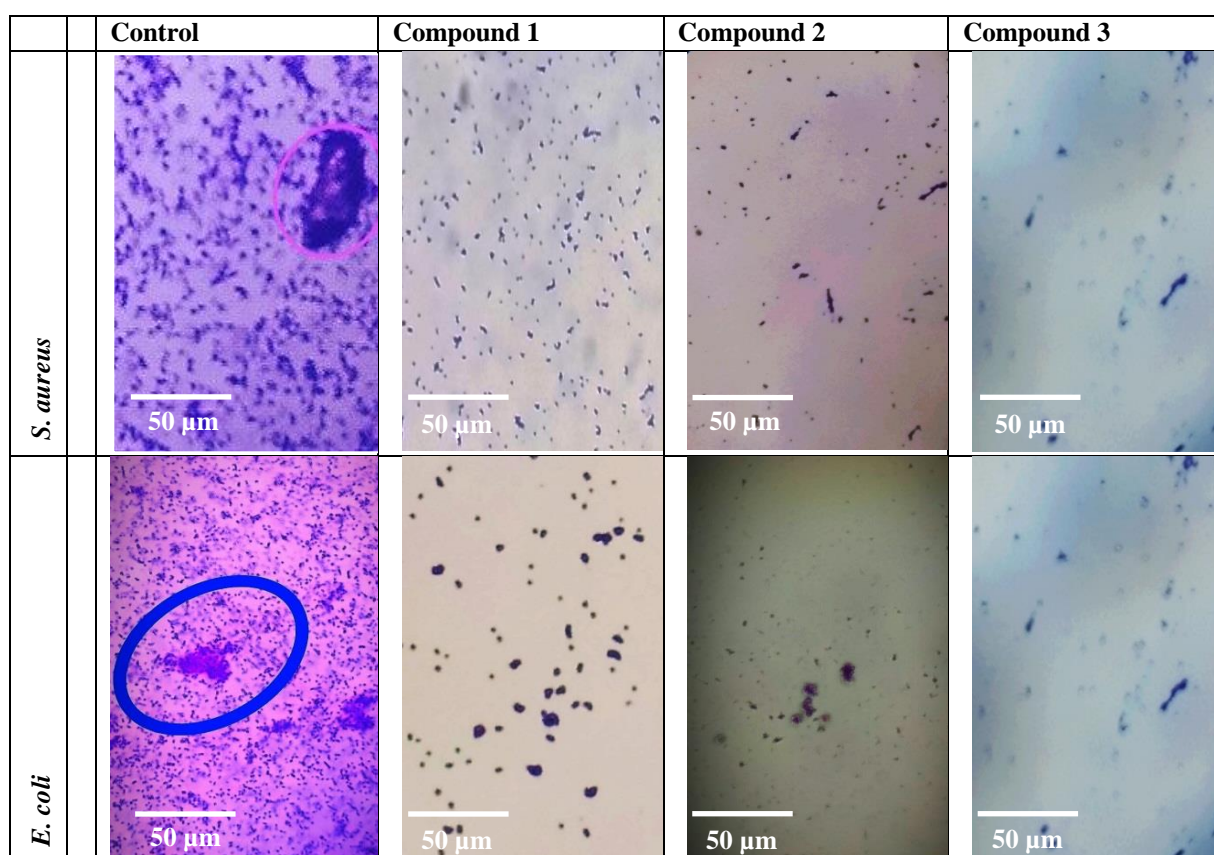
Fig. 3. Light microscopy images of biofilm inhibition in the absence and presence of tetracenomycin D (**1**), resistomycin (**2**), and resistoflavin (**3**) against *S. aureus* and *E. coli*.
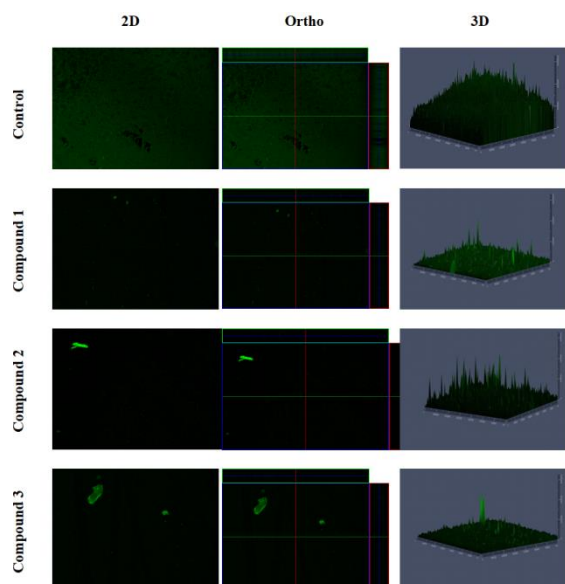

Fig. 4. CLSM of biofilms formed by *S. aureus* treated with tetracenomycin D (**1**), resistomycin (**2**), and resistoflavin (**3**) at a 200 µg/ml.
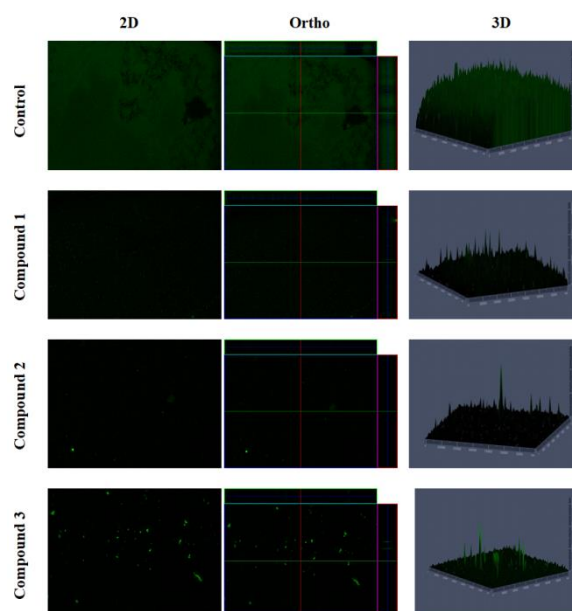

Fig. 5. CLSM of biofilms formed by *E. coli* treated with tetracenomycin D (**1**), resistomycin (**2**), and resistoflavin (**3**) at 200 µg/ml.
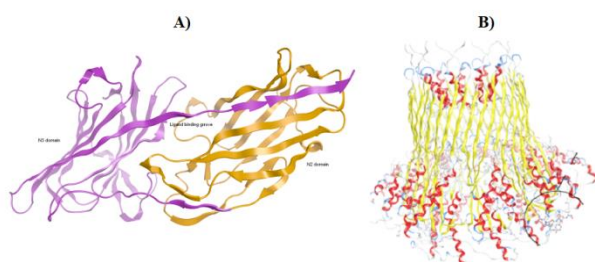
Fig. 6. Structural organization of ClfB (A) and CsgG (B).

Hence, the isolated metabolites (**1-3**) were docked at the binding grooves of ClfB and CsgG, and the significant molecular interactions were illustrated in Figures 7, 8a and 8b and summarized in Table 1.

In the case of ClfB protein, tetracenomycin D (**1**) was inserted between β-strand E of N2 domain and β-strand B of N3 domain and oriented in its planar configuration with an intramolecular H-bonding to probe interactions with amino acids in its proximity. The main chain Arg529 NH showed two polar hydrogen-pi (Hp-π) interactions with rings A and B of tetracenomycin D, while the phenyl side chain of Phe328 in N2 domain was T-stacked with ring B. Furthermore, polar interactions were observed between tetracenomycin D and Pro233 and Asp270 residues. The backbone amide oxygen of Pro233 accepted a H-bonding from the phenolic group of ring D and backbone amide NH donates a H-bonding to the quinoid oxygen of ring C. Resistomycin (**2**) is sandwiched between N2 loop and N3 β-strand F, where the side chain phenolic group of Tyr273 donates a H-bonding interaction with the anthrone carbonyl oxygen of resistomycin, and phenol side chain of Tyr530 exhibited -π—π stacking of the aromatic scaffold of resistomycin. Compound **3**, resistoflavin, was oriented in the binding pocket to establish two polar interactions with Thre383 and Arg 529 residues. The phenolic OH donates an H-bonding to the side chain OH of Thre383, while the alcoholic OH donates an H-bonding to the main chain carbonyl oxygen of Arg529. Altogether, the coplanarity of the isolated metabolites' core scaffold and oxygenated probes (i.e. alcoholic, phenolic, and carbonyl) are essential pharmacophores for efficient binding at the N2-N3 trench. This provides an initial basis for the molecular recognition of small molecules binding to ClfB cell adhesion protein and paves the road for extensive research to discover potent ClfB inhibitors.

In the case of lipoprotein CsgG found in the outer membrane of pathogenic Enterobacteriaceae, including *E. coli*, is a highly specialized nanomeric channel secretion system that is responsible for transporting curli proteins into the extracellular matrix to form highly agglomerated and clustered amyloid fibrils [38,39]. These pathogenic curli amyloids promote biofilm establishment to protect bacterial cells from host immune responses and antimicrobial therapeutics [40,41]. As shown in Figure 8, tetracenomycin D (**1**) was extended at the binding pocket of CsgG, forming an intramolecular hydrogen bonding between its phenolic OH and the carbonyl oxygen of its quinone moiety. Tetracenomycin D (**1**) also showed an arene-H interaction with the backbone amide hydrogen of Asn109 (Figure 8), with a total binding score of -4.9 (Table 1). Interestingly, Tyr6 of CsgAN6 peptide substrate was bounded similarly to Asn109 of CsgG subunit, augmenting our modelling study [35]. Resistomycin (**2**) occupied the binding crevice at the same chemical environments as tetracenomycin D (**1**). It exhibited arene-H interaction with Asn108 CsgG curli subunit and experienced hydrophobic interaction with side chains of Ile34 and Iles121, as shown in Figure 8, and the docking score for was found -4.9 (Table 1). Consequently, the docking study revealed unique binding modes of the isolated metabolites and their interactions with critical amino acids at the CsgG subunit, thus promoting in vitro validation. Lastly, resistoflavin (**3**) occupied at the binding groove with a slightly curved orientation, where it donates a hydrogen bond to the Thr31 main chain amide nitrogen of CsgG subunit (Figure 8). In addition, the two geminal methyl groups were docked at a shallow hydrophobic sub-pocket created by side chains of amino acids Ile34, Ile121, and Trp237. In addition, the overall binding score was found as -4.8. Intestinally, Trp237 was also found in proximity to the hydrophobic isopropyl group of side chain Val 2 of the CsgAN6 peptide substrates, further validating our docking models.
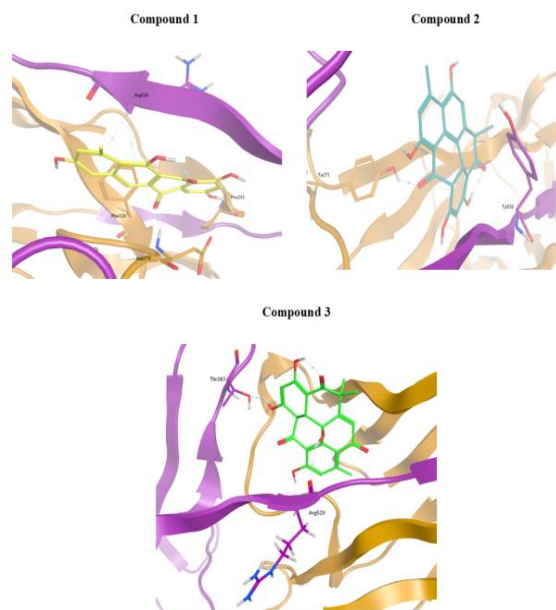

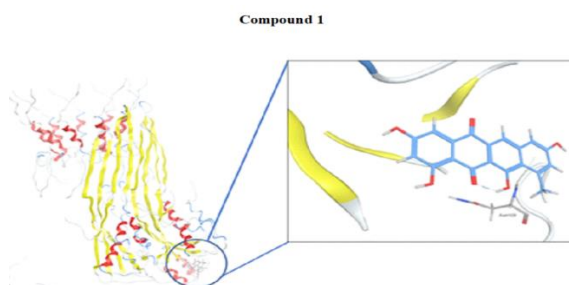Fig. 7. The binding modes of compounds **1-3** at ClfB binding groove.

Compound 1

Fig. 8a. Binding mode of compound **1** at CsgG binding groove
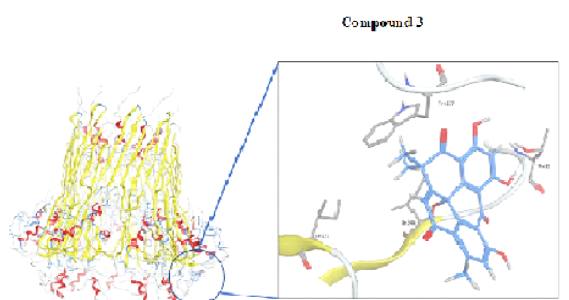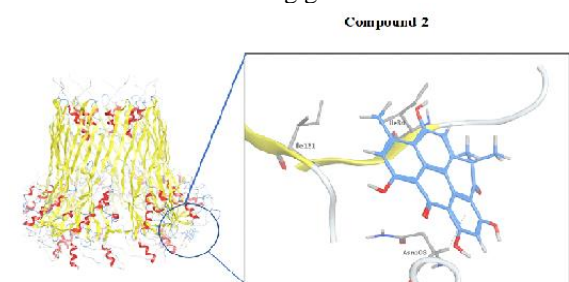
Compound 2

Compound 3

Fig. 8b. The binding modes of compounds **1**-**3** at CsgG binding groove

4. Conclusion

The antibiofilm activity of three pigmented secondary metabolites **1**-**3** was investigated. To the best of our knowledge, this is the first report showing the possible antibiofilm activity of, tetracenomycin D (**1**), resistomycin (**2**), and resistoflavin (**3**) produced by *Streptomyces* sp. EG1. Compounds **1**-**3** at concentrations ranging from 100 to 400 μg/ml are required to interrupt the 3D architecture of bacteria and reduce the biofilm formation created by *S. aureus* and *E. Coli*. Furthermore, a docking study revealed unique binding modes of the isolated metabolites **1**-**3** with critical amino acids of the biofilm forming protein ClfB in *Staphylococcus aureus* and the CsgG subunit in *E. Coli*, thus promoting *in vitro* validation. These isolated compounds add to the evidence that marine actinomycetes are a good source of bioactive compounds with antibiofilm activity.

5. Conflicts of interest

The authors declare that there are no conflicts of interest.

6. Acknowledgments

Table 1. Molecular interactions of metabolites (**1**-**3**) with amino acids of ClfB and CsgG, and their docking scores

Metabolite	ClfB		CsgG	
	Docking Score (Kcal/mol)	Interacting amino acids	Docking Score (Kcal/mol)	Interacting amino acids
Tetracenomycin D (**1**)	- 5.4	Arg529, Pro233, ASP and Phe328	-4.9	Asn109, Ile34, Ile121, and Trp237
Resistomycin (**2**)	- 5.6	Thre383 and Arg529	-4.9	Asn108, Ile34, and Ile121
Resistofalvin (**3**)	- 5.3	Try273 and Try530	-4.8	Thre31

7. References

[1] S. Haruta, N. Kanno, Survivability of microbes in natural environments and their ecological impacts, Microbes Environ. 30 (2015) 123–125. doi:10.1264/jsme2.ME3002rh.

[2] H.C. Flemming, S. Wuertz, Bacteria and archaea on Earth and their abundance in biofilms, Nat. Rev. Microbiol. 17 (2019) 247–260. doi:10.1038/s41579-019-0158-9.

[3] S. Doron, S.L. Gorbach, Bacterial Infections: Overview, Int. Encycl. Public Heal. (2008) 273. doi:10.1016/B978-012373960-5.00596-7.

[4] R.M. Donlan, Biofilms: Microbial Life on Surfaces, Emerg. Infect. Dis. 8 (2002) 881. doi:10.3201/EID0809.020063.

[5] A. Schulze, F. Mitterer, J.P. Pombo, S. Schild, Biofilms by bacterial human pathogens: Clinical relevance - Development, composition and regulation - Therapeutical strategies, Microb. Cell. 8 (2021) 28–56. doi:10.15698/MIC2021.02.741.

[6] R. Mishra, A.K. Panda, S. De Mandal, M. Shakeel, S.S. Bisht, J. Khan, Natural Anti-biofilm Agents: Strategies to Control Biofilm-Forming Pathogens, Front. Microbiol. 11 (2020) 2640. doi:10.3389/FMICB.2020.566325/BIBTEX.

[7] M. Jamal, W. Ahmad, S. Andleeb, F. Jalil, M. Imran, M.A. Nawaz, T. Hussain, M. Ali, M. Rafiq, M.A. Kamil, Bacterial biofilm and

_____

associated infections, J. Chinese Med. Assoc. 81 (2018) 7–11. doi:10.1016/j.jcma.2017.07.012.

[8] Z. Khatoon, C.D. McTiernan, E.J. Suuronen, T.F. Mah, E.I. Alarcon, Bacterial biofilm formation on implantable devices and approaches to its treatment and prevention, Heliyon. 4 (2018) e01067. doi:10.1016/j.heliyon.2018.e01067.

[9] S. Veerachamy, T. Yarlagadda, G. Manivasagam, P.K. Yarlagadda, Bacterial adherence and biofilm formation on medical implants: A review, Proc. Inst. Mech. Eng. Part H J. Eng. Med. 228 (2014) 1083–1099. doi:10.1177/0954411914556137.

[10] E.C. von Rosenvinge, G.A. O'May, S. Macfarlane, G.T. Macfarlane, M.E. Shirtliff, Microbial biofilms and gastrointestinal diseases, Pathog. Dis. 67 (2013) 25–38. doi:10.1111/2049-632X.12020.

[11] S.L. Percival, S.M. McCarty, B. Lipsky, Biofilms and Wounds: An Overview of the Evidence, Adv. Wound Care. 4 (2015) 373. doi:10.1089/WOUND.2014.0557.

[12] M. Brandwein, D. Steinberg, S. Meshner, Microbial biofilms and the human skin microbiome, Npj Biofilms Microbiomes 2016 21. 2 (2016) 1–6. doi:10.1038/s41522-016-0004-z.

[13] J. Barros, L. Grenho, S. Fontenente, C.M. Manuel, O.C. Nunes, L.F. Melo, F.J. Monteiro, M.P. Ferraz, *Staphylococcus aureus* and *Escherichia coli* dual-species biofilms on nanohydroxyapatite loaded with CHX or ZnO nanoparticles, J. Biomed. Mater. Res. - Part A. 105 (2017) 491–497. doi:10.1002/jbm.a.35925.

[14] Z. Sedarat, A.W. Taylor-Robinson, Biofilm Formation by Pathogenic Bacteria: Applying a *Staphylococcus aureus* Model to Appraise Potential Targets for Therapeutic Intervention, Pathogens. 11 (2022). doi:10.3390/pathogens11040388.

[15] S. Divakar, M. Lama, K. Asad U., Antibiotics versus biofilm: an emerging battleground in microbial communities | Enhanced Reader, Antimicrob. Resist. Infect. Control. 8 (2019) 1–10.

[16] L.K. Vestby, T. Grønseth, R. Simm, L.L. Nesse, Bacterial Biofilm and its Role in the Pathogenesis of Disease, Antibiotics. 9 (2020). doi:10.3390/ANTIBIOTICS9020059.

[17] M. Jamal, W. Ahmad, S. Andleeb, F. Jalil, M. Imran, M.A. Nawaz, T. Hussain, M. Ali, M. Rafiq, M.A. Kamil, Bacterial biofilm and associated infections, J. Chinese Med. Assoc. 81 (2018) 7–11. doi:10.1016/j.jcma.2017.07.012.

[18] M.S. Abdelfattah, K. Toume, M. Ishibashi, Izumiphenazine D, a new phenazoquinoline N-

[19] oxide from *Streptomyces* sp. IFM 11204, Chem. Pharm. Bull. 59 (2011) 508–510. doi:10.1248/cpb.59.508.

[19] M.S. Abdelfattah, J. Rohr, Premithramycinone G, an early shunt product of the mithramycin biosynthetic pathway accumulated upon inactivation of oxygenase MtmOII, Angew. Chemie - Int. Ed. 45 (2006) 5685–5689. doi:10.1002/anie.200600511.

[20] M.S. Abdelfattah, M.A. Arai, M. Ishibashi, Bioactive secondary metabolites with unique aromatic and heterocyclic structures obtained from terrestrial actinomycetes species, Chem. Pharm. Bull. 64 (2016) 668–675. doi:10.1248/cpb.c16-00038.

[21] Yixizhuoma, N. Ishikawa, M.S. Abdelfattah, M. Ishibashi, Elmenols C-H, new angucycline derivatives isolated from a culture of *Streptomyces* sp. IFM 11490, J. Antibiot. (Tokyo). 70 (2017) 601–606. doi:10.1038/ja.2016.158.

[22] M.C. Kim, R. Cullum, A.M.S. Hebishy, H.A. Mohamed, A.H.I. Faraag, N.M. Salah, M.S. Abdelfattah, W. Fenical, Mersaquinone, a new tetracene derivative from the marine-derived *Streptomyces* sp. EG1 exhibiting activity against methicillin-resistant *Staphylococcus aureus* (MRSA), Antibiotics. 9 (2020). doi:10.3390/antibiotics9050252.

[23] M.S. Abdelfattah, R.P. Maskey, R.N. Asolkar, I. Grün-Wollny, H. Laatsch, **S**eitomycin: isolation, structure elucidation and biological activity of a new angucycline antibiotic from a terrestrial Streptomycete, J. Antibiot. 56 (2003) 539–542. doi: 10.7164/antibiotics.56.539.

[24] A.S. Azman, C.I. Mawang, J.E. Khairat, S. AbuBakar, Actinobacteria—a promising natural source of anti-biofilm agents, Int. Microbiol. 22 (2019) 403–409. doi:10.1007/s10123-019-00066-4.

[25] P. Deka, Zothanpuia, A.K. Passari, B.P. Singh, Actinobacteria as a potential natural source to produce antibiofilm compounds: An overview, Elsevier B.V., 2019. doi:10.1016/B978-0-444-64279-0.00007-4.

[26] V. Ramalingam, D. Mahamuni, R. Rajaram, In vitro and in silico approaches of antibiofilm activity of 1-hydroxy-1-norresistomycin against human clinical pathogens, Microb. Pathog. 132 (2019) 343–354. doi:10.1016/j.micpath.2019.05.021.

[27] S.E.A. Badr, M.S. Abdelfattah, S.H. El-Sayed, A.S.E. Abd El-Aziz, D.M. Sakr, Evaluation of anticancer, antimycoplasmal activities and chemical composition of guar (Cyamopsis tetragonoloba) seeds extract, Res. J. Pharm. Biol. Chem. Sci. 5 (2014) 413–423.

[28] E.F. Haney, M.J. Trimble, R.E.W. Hancock, Microtiter plate assays to assess antibiofilm

activity against bacteria, Nat. Protoc. 16 (2021) 2615–2632. doi:10.1038/S41596-021-00515-3.

[29] R.T. Merod, J.E. Warren, H. McCaslin, S. Wuertz, Toward Automated Analysis of Biofilm Architecture: Bias Caused by Extraneous Confocal Laser Scanning Microscopy Images, Appl. Environ. Microbiol. 73 (2007) 4922. doi:10.1128/AEM.00023-07.

[30] I. Kock, R.P. Maskey, M.A.F. Biabani, E. Helmke, H. Laatsch, 1-Hydroxy-1-norresistomycin and Resistoflavin Methyl Ether: New Antibiotics from Marine-derived Streptomycetes. J. Antibiot. (Tokyo). 58 (2005) 530–534. doi:10.1038/ja.2005.73.

[31] M.S. Abdelfattah, M.I.Y. Elmallah, A.H.I. Faraag, A.M.S. Hebishy, N.H. Ali, Heliomycin and tetracinomycin D: anthraquinone derivatives with histone deacetylase inhibitory activity from marine sponge-associated *Streptomyces* sp. SP9, 3 Biotech. 8 (2018). doi:10.1007/s13205-018-1304-1.

[32] Z. Song, J. Zhang, K. Zhou, L. Yue, Y. Zhang, J.A. Jennings, K. Wang, Anthraquinones as Potential Antibiofilm Agents Against Methicillin-Resistant *Staphylococcus aureus*, 12 (2021) 1–16. doi:10.3389/fmicb.2021.709826.

[33] H. Xiang, Y. Feng, J. Wang, B. Liu, Y. Chen, L. Liu, X. Deng, M. Yang, Crystal structures reveal the multi-ligand binding mechanism of *Staphylococcus aureus* ClfB, PLoS Pathog. 8 (2012). doi:10.1371/journal.ppat.1002751.

[34] P. Goyal, P. V. Krasteva, N. Van Gerven, F. Gubellini, I. Van Den Broeck, A. Troupiotis-Tsaïlaki, W. Jonckheere, G. Péhau-Arnaudet, J.S. Pinkner, M.R. Chapman, S.J. Hultgren, S. Howorka, R. Fronzes, H. Remaut, Structural and mechanistic insights into the bacterial amyloid secretion channel CsgG, Nature. 516 (2014) 250–253. doi:10.1038/nature13768.

[35] N. Van Gerven, R.D. Klein, S.J. Hultgren, H. Remaut, Bacterial amyloid formation: Structural insights into curli biogensis, Trends Microbiol. 23 (2015) 693–706. doi:10.1016/j.tim.2015.07.010.

[36] P. Rattu, F. Glencross, S.L. Mader, C.K. Skylaris, S.J. Matthews, S.L. Rouse, S. Khalid, Atomistic level characterisation of ssDNA translocation through the E. coli proteins CsgG and CsgF for nanopore sequencing, Comput. Struct. Biotechnol. J. 19 (2021) 6417–6430. doi:10.1016/J.CSBJ.2021.11.014.

[37] C.C.S. Deivanayagam, E.R. Wann, W. Chen, M. Carson, K.R. Rajashankar, M. Höök, S.V.L. Narayana, A novel variant of the immunoglobulin fold in surface adhesins of *Staphylococcus aureus*: Crystal structure of the fibrinogen-binding MSCRAMM, clumping factor A, EMBO J. 21 (2002) 6660–6672. doi:10.1093/emboj/cdf619.

[38] B. Cao, Y. Zhao, Y. Kou, D. Ni, X.C. Zhang, Y. Huang, Structure of the nonameric bacterial amyloid secretion channel, Proc. Natl. Acad. Sci. U. S. A. 111 (2014) E5439–E5444. doi:10.1073/PNAS.1411942111/-/DCSUPPLEMENTAL.

[39] L.S. Robinson, E.M. Ashman, S.J. Hultgren, M.R. Chapman, Secretion of curli fibre subunits is mediated by the outer membrane-localized CsgG protein, Mol. Microbiol. 59 (2006) 870–881. doi:10.1111/j.1365-2958.2005.04997.x.

[40] M.M. Barnhart, M.R. Chapman, Curli biogenesis and function, Annu. Rev. Microbiol. 60 (2006) 131–147. doi:10.1146/annurev.micro.60.080805.142106.

[41] N. Jain, J. Ådén, K. Nagamatsu, M.L. Evans, X. Li, B. McMichael, M.I. Ivanova, F. Almqvist, J.N. Buxbaum, M.R. Chapman, Inhibition of curli assembly and *Escherichia coli* biofilm formation by the human systemic amyloid precursor transthyretin, Proc. Natl. Acad. Sci. U. S. A. 114 (2017) 12184–12189. doi:10.1073/pnas.1708805114.